

Analytical Methods

Accepted Manuscript



This is an *Accepted Manuscript*, which has been through the Royal Society of Chemistry peer review process and has been accepted for publication.

Accepted Manuscripts are published online shortly after acceptance, before technical editing, formatting and proof reading. Using this free service, authors can make their results available to the community, in citable form, before we publish the edited article. We will replace this *Accepted Manuscript* with the edited and formatted *Advance Article* as soon as it is available.

You can find more information about *Accepted Manuscripts* in the [Information for Authors](#).

Please note that technical editing may introduce minor changes to the text and/or graphics, which may alter content. The journal's standard [Terms & Conditions](#) and the [Ethical guidelines](#) still apply. In no event shall the Royal Society of Chemistry be held responsible for any errors or omissions in this *Accepted Manuscript* or any consequences arising from the use of any information it contains.

1
2
3 **Development of a photometric procedure for tin determination in canned**
4 **foods employing a multicommuted flow analysis approach**
5
6
7

8 Tuanne R. Dias, Boaventura F. Reis¹
9

10
11 Centro de Energia Nuclear na Agricultura, Universidade de São Paulo
12 Av. Centenário, 303, São Dimas, CEP 13400 970, Piracicaba - SP, Brazil
13
14

15
16 **Abstract**
17

18 This work describes an automated analytical procedure for the photometric
19 determination of tin in canned foods, employing a multicommuted flow analysis
20 process. The flow system manifold comprised a set of three-way solenoid
21 valves to handle solutions and a multisyringe module for fluid propelling. A PIC
22 microcontroller, running a software written in Visual Basic 6.0 language was
23 used to control the flow analysis setup and to perform data acquisition.
24 Photometric detection was accomplished employing a homemade photometer,
25 which consisted of an ultra-bright LED, a photodiode and a homemade flow cell
26 with optical path length of 200 mm. The procedure was based on the reaction
27 of Sn(IV) with pyrocatechol violet (PCV) in the presence of surfactants. After
28 selecting the best operational conditions, profitable features such as, a linear
29 response ranging from 0.10 to 1.25 mg L⁻¹, a limit of detection 0.04 mg L⁻¹, a
30 variation coefficient of 1.30 % (n =10) and a sampling rate of 49 determination
31 per hour were achieved. By spiking samples with tin, recoveries between 95
32 and 110% were achieved.
33
34
35
36
37
38
39
40
41
42
43

44
45 **Keywords:** Multicommuted flow analysis, Spectrophotometry, Long pathlength
46 flow cell, LED based photometer, Tin, Food.
47
48

49
50
51 ¹Corresponding author: Tel. +55 19 3429 4639.

52
53 E-mail address: reis@cena.usp.br (B.F. Reis).
54
55
56
57
58
59
60

1. Introduction

Tin exist in oxidation states II and IV.¹ State II is more toxic and unstable, because it can easily be converted to IV.² In nature, tin occurs mainly in the form of cassiterite (SnO_2), which is insoluble in water and has low toxicity.³ Tin organic compounds can occur through the methylation of inorganic forms by microorganisms, converting them to toxic organic compounds.⁴

Tin has been extensively used in various applications, including in pigments, glass coating, dental fluoridation, electronic devices, stabilizers (e.g. PVC)^{5,6} and for the production of fungicides and bactericides.² Besides these applications, the main industrial use of tin has been to produce tinplate for food and beverage packing. According to a review presented by S. Blunden & Wallace,⁷ 20% of the tin processed per year in Europe is used to produce cans for food packing.

Because tin can accumulate in the human body,⁸ special attention has been given to tin use in the internal lining of cans for storing drinks and foods, as this is considered one of the main sources of contamination for humans.⁷ Depending on the composition and characteristics of the canned foods, including acidity, oxidizing agents (anthocyanins, iron, etc.), the presence of oxygen in the package, time and storage conditions, the leaching of tin to the food may occur.^{9,10}

Although inorganic tin is poorly absorbed by the gastrointestinal tract, tin can accumulate in the tissues. The half-life of tin in the organism is considerably long (29 days),¹¹ which makes it a risk for human health, as tin is not considered an essential element. There are indications that a number of diseases, including gastrointestinal disturbances, abdominal pain, diarrhea, nausea, vomit, anemia, liver diseases, and kidney failure have been caused by contamination by tin. In the case of tin organic compounds, due to their toxicity, the effects are more pronounced e.g. encephalopathy, central nervous system disorder and brain edema, which can be caused by the triethyltin compound.^{5,7,12}

Leaching of metallic tin from food storage cans can occur, and the tin may be ingested in its divalent state,⁷ which is the most aggressive. Because of this, the Brazillian Health Surveillance Agency (ANVISA)¹³ prohibits the use of tin solder in packaging, except for dehydrated products. The European

1
2
3 Community Regulatory Commission¹⁴ established that the maximum amount
4 permissible of inorganic tin is 100 mg kg⁻¹ for canned beverages and 200 mg
5 kg⁻¹ for canned foods.
6
7

8 According to the World Health Organization (WHO) guidelines,¹⁵ the
9 tolerable intake of tin concentration per week is 14 mg kg⁻¹ or 120 mg per day,
10 for an adult weighing 60 kg. Therefore, tin determination in canned foods is
11 essential to ascertain the quality. Towards this, the literature reports a number
12 of methods for tin determination, employing as detection techniques inductively
13 coupled plasma optical emission spectrometry,¹⁶ graphite furnace absorption
14 atomic spectrometry,¹⁷ spectrophotometry¹⁸ and inductively coupled plasma
15 mass spectrometry.¹⁹ Among these detection techniques, spectrophotometry
16 uses the most cost-effective equipment. Most of the published papers focused
17 on tin determination by spectrophotometry were implemented using batch
18 approaches.^{20,21} The referred procedures, performed manually, are time-
19 consuming and require large volumes of sample and reagent solutions,^{6,20,21}
20 which is a disadvantage, thus a resource to overcome this drawback would be
21 welcome.
22
23
24
25
26
27
28
29
30

31 The Flow injection analysis (FIA) process,²² mainly the branches known
32 as sequential analysis (SIA)²³, multicommuted flow analysis (MCFA)²⁴,
33 multisyringe flow-injection analysis (MSFIA)^{25,26} and multi-pumping flow analysis
34 (MPFA)^{27,28} provide analytical procedures that can save time and reagents,
35 thus complying with green chemistry recommendations.^{29,30}
36
37
38
39

40 Intending to develop an automated analytical procedure for photometric
41 determination of tin in canned foods, focused on saving sample and reagent
42 solutions, we selected the multicommuted flow analysis process to implement
43 the analytical procedure. The flow analysis module was designed to use a
44 syringe pump to propel the solution and a set of solenoid valves to handle
45 sample and reagent solution, controlled using a PIC microcontroller. The
46 analytical procedure was developed to exploit the tin reaction with pyrocatechol
47 violet (PCV), which forms a compound that absorbs radiation at 550 nm.³¹ This
48 compound in surfactant medium undergoes a wavelength shift towards a higher
49 wavelength,³² a resource exploited in this work to improve sensitivity.
50
51
52
53
54
55
56
57
58
59
60

1
2
3 In order to achieve high sensitivity without resorting to any pre-
4 concentration stage, we used a homemade LED photometer, designed to allow
5 the use of a flow cell with an optical pathlength of 200 mm.
6
7

8 9 10 **2.Experimental**

11 12 *2.1.Reagents and solutions*

13 All reagents used were of analytical grade. Purified water with electrical
14 conductivity less than $0.1 \mu\text{S cm}^{-1}$ was used throughout. A 0.10% (w/v)
15 pyrocatechol violet (PCV) stock solution (Merck) was prepared by dissolving
16 0.050 g of solid in 50 mL of water. Working solution 0.04% (w/v) PCV was
17 prepared by dilution with water from the stock.
18
19

20 Glycine buffer solutions 1.0 mol L^{-1} with pH ranging from 1.63 to 2.68
21 were prepared by dissolving the appropriated amount of solid reagent (Merck)
22 in 100 mL of water. After dissolution, the pH was adjusted to 2.0 with
23 hydrochloric acid and volume was completed to 200 mL with water.
24
25

26 A 1.0% (v/v) tween-80 stock solution was prepared by dissolving 1.0 g of
27 solid (Quimex) in 100 mL of water. A 0.40% (w/v) cetyltrimethylammonium
28 bromide (CTAB) stock solution was prepared by dissolving 0.4 g CTAB in 100
29 mL of water. The surfactant working solution (0.10 % tween-80 plus 0.16 %
30 CTAB) was prepared by mixing 10 mL of tween-80 and 40 mL CTAB solutions
31 and completing the volume to 100 mL with water.
32
33

34 A 1.0000 gL^{-1} Sn(IV) stock solution was prepared by weighing 0.2950 g
35 of $\text{SnCl}_4 \cdot 5\text{H}_2\text{O}$ (Merck) and dissolving it in 100 mL of a 2.0 mol L^{-1} hydrochloride
36 acid solution. Working standard solutions of Sn(IV) with concentrations ranging
37 from 0.10 to 2.50 mg L^{-1} in a 0.5 mol L^{-1} HCl were prepared daily by dilution
38 from a 20 mg L^{-1} Sn(IV) stock solution previously prepared.
39
40

41 To study the interference effect that would be caused by the concomitant
42 ions, assays were implemented using standard solutions containing 0.5 mg L^{-1}
43 Sn(IV) and different concentrations of the potential interfering species. A
44 solution of 0.5 mg L^{-1} Sn(IV) without the potential interfering species was used
45 as a reference solution.
46
47
48
49
50
51
52
53
54
55

56 57 58 *2.2.Sample preparation*

59
60

1
2
3 Samples of green corn, tomato extract, and tomato without skin were
4 ground using a mill (Q-298A, Quimis). Tuna samples were macerated using a
5 mortar and pestle. Sample decomposition was performed employing a
6 microwave-assisted methodology carried out using a microwave oven (ETHOS
7 1600, Milestone). Three amount of 0.2 g of each sample were accurately
8 weighted and placed into the digesting vessels. Afterwards, to the vessels were
9 added 6.0 mL of a mix of acids previously prepared by mixing 48 mL HCl (12
10 mol L⁻¹) and 16 mL HNO₃ (14 mol L⁻¹) diluted to 200 mL with water. After
11 digesting and cooling to the laboratory temperature (22 °C), the volume was
12 completed to 50 mL with water.
13
14
15
16
17
18

19 Prior to the sample digesting step, assays were accomplished in order to
20 verify if the cans had or not a tin coating. The assays were carried out using a
21 laser-induced breakdown spectroscopy (LIBS) setup ((Brilliant, Quantel,
22 France), furnished with a Nd:YAG 1064 nm laser with 100 mJ pulse energy,
23 which was operated settling a delay time of 2.0 μs to start the readings and an
24 integration time of 5.0 μs for signal acquisition. The pulses of laser were
25 focused on the sample surface (can fragment) and the plasma emission was
26 focused on the input optical fiber of a LLA ESA3000 model spectrometer.
27
28
29
30
31
32
33

34 *2.3. Setups description and accessories*

35
36 The syringe pump employed for solution propulsion (Crison, 4S) has a
37 mechanism, controlled by a stepping motor that allows the simultaneous
38 displacement of the pistons. For full piston displacement, (forward or backward)
39 the equipment performed by default 40,000 steps. The smallest volume that
40 could be delivered was 0.25 μL, when using a syringe with a volume of 10 mL.
41 Flow rates can be selected within the range of 1 to 30 mL min⁻¹. The flow rate
42 and solution volumes to be delivered were previously preset and sent by the
43 microcontroller to the syringe module through the RS232 serial interface.
44
45
46
47
48

49 A microcontroller PIC18F4550 (Microgênios, São Paulo, Brazil) was
50 employed to control the flow system module and to perform data acquisition.
51 This microcontroller has digital interfaces and an analogical to digital converter
52 with 12 bits of resolution (4096 mV full scale). The microcontroller was
53 configured to operate as a “slave” under the directive of a microcomputer
54
55
56
57
58
59
60

1
2
3 communicated through a serial interface, which was accomplished by running
4 software written in Visual Basic 6.0 (Microsoft).

5
6 The photometer comprised a flow cell with an optical path length of 200
7 mm, a 5 mm ultra bright red LED, maximum emission at 630 nm and beam
8 opening angle of 23°; and a photodiode OPT301 (Texas Instruments) with
9 amplification network coupled to the transduction unit. Other electronic devices
10 required consisted of a regulated power supply 12 V to provide energy for
11 solenoid valves; a regulated power supply (-12 V, + 12 V) to feed the
12 photometer; a digital control interface based on the integrated circuit ULN2803
13 to drive solenoid valves, wired as described elsewhere,³³ a transistor BD547
14 and resistors to control LED emission intensity.

15
16 The LED based photometer was designed in order to allow the use of a
17 flow cell with an optical pathlength of 200 mm, molded as described in a
18 previous work³⁴ and the photometer assembling is depicted in Fig.1.

19
20
21
22
23
24
25
26
27
28 Figure 1

29
30
31 The radiation beam (I_1) emitted by the LED is collected by the glass
32 cylinder (gc), which works as a wave guide, directing the radiation beam to
33 inside of flow cell. At the other end of the flow cell, the glass cylinder (gc)
34 collects the radiation beam (I_2) and focuses it on the observation windows of the
35 photodetector (Det). When the flow cell is filled with water, the intensities of both
36 radiation beams are practically equal, but when the flow cell is filled with a
37 solution that absorbs radiation, the intensity of the radiation beam (I_2) becomes
38 smaller. The photodetector (OPT301) has a linear relationship with the intensity
39 of the radiation beam (I_2), a feature that is exploited for absorbance calculation.
40 The intensity of the radiation beam is controlled by mean of the variable resistor
41 wired to the base of the transistor (Tr), thus allowing easy adjustment of the full
42 scale measurement.

43
44 The photometric procedure for tin determination exploits the reaction of
45 Sn(IV) with pyrocatechol violet (PCV) in a glycine buffered medium. Considering
46 these requirements for reaction development, we designed the flow analysis
47 module shown in Fig.2.

1
2
3
4
5
6
7
8
9
10
11
12
13
14
15
16
17
18
19
20
21
22
23
24
25
26
27
28
29
30
31
32
33
34
35
36
37
38
39
40
41
42
43
44
45
46
47
48
49
50
51
52
53
54
55
56
57
58
59
60

Figure 2

This flow system is based on the multicommutated flow analysis process,³³ designed to employ a multisyringe pump for fluid propelling, which was programmed to work maintaining a flow rate of 3.0 mL min⁻¹.

2.4. Procedure development

Prior to starting the analytical run, the photometer calibration step was performed as follows. Maintaining the flow cell filled with the carrier fluid, the LED illumination was increased up to the signal generated by the photometer attained the full scale-value ($S_v = 4000$ mV). This signal read by the microcontroller was converted to digital and sent to the microcomputer. This adjustment was made by manipulating the variable resistor wired to the base transistor (Tr, Fig. 1). Afterward, the flow cell was filled with Sn(IV)-PCV complex solutions, previously prepared using two Sn(IV) standard solutions with concentrations of 100 and 150 mgL⁻¹. The signals generated by the photometer related to these solutions were practically equal (90.2, 91.1 mV), which was considered as the residual measurements (R_s).³⁴ The full scale and residual measurements (S_v , R_s) were saved to be used for absorbance calculation. In a previous work,³⁴ it was proved that for LED based photometer, furnished with flow cell of long pathlength and tubular geometry, better adherence to the Bouguer-Lambert-Beer law was achieved using the residual measurement (R_s), instead of the usual dark measurement.³⁵

The calibration step was performed 20 min after powering the photometer. Taking into account that the monitored compound absorbs radiation obeying the Bouguer-Lambert-Beer' law, absorbance was calculated using the following relationship.³⁴

$$\text{Absorbance} = \log(S_v - R_s) / (V_i - R_s)$$

Where:

S_v = full scale measurement (4000 mV)

R_s = residual measurement

V_i = current measurement

Analyzing the calibration results achieved over one week, we observed that when the full-scale value was maintained closed to 4000 mV, the residual measurement (R_s) did not vary significantly. Based on these results, the R_s value was updated once per week.

After the calibration step, the procedure for tin determination was carried out following the steps described in Table 1. Under the microcomputer directive, the microcontroller sent a command signal to enable the syringe pump to carry out the aspiration action. Afterwards, the sampling step was performed by switching on valves V_1 and V_{B4} , thus an aliquot of sample solution was aspirated to fill the sampling loop (B_1). After a preset time interval (Δt), a new command was sent to the syringe pump to revert the pumping direction. Valves V_{B1} , V_{B2} and V_{B3} were maintained switched on, while valves V_2 and V_3 were switched on/off alternately for a number of preset times. These were done to load the coil (B_2) with a mix of chromogenic reagent (PCV) and surfactant solutions. Afterward, the sample aliquot was displaced from the sampling loop (B_1) by the glycine buffer solution merging with PCV solution at the joint device (C_3). After a preset time interval to load the reaction coil (B_3) with the mixture comprising sample, PCV and surfactant solutions, a signal command was sent by the microcontroller to stop the pumping solutions and to switch off all valves. After a time interval for reaction development, the syringe piston displacement was enabled and valve V_{B3} was switched on, thus the complex formed was displaced by the carrier buffer solution toward the photodetector (Det). The signal generated by the photometer was converted to digital by the microcontroller and sent to microcomputer and saved as an ASCII file to allow further processing. While the analytical run proceeded, a plot of the signal was displayed on the microcomputer screen as a time function, thus allowing its visualization in real time.

Table 1. Sequence of events to perform an analytical run

Step	Actuation							n° of steps	Pumping direction
	V_1	V_2	V_3	V_{B1}	V_{B2}	V_{B3}	V_{B4}		
Sampling	1	0	0	0	0	0	1	1500	Backward
Reagent addition	0	0/1	1/0	1	1	1	0	1200	Forward

Stopped	0	0	0	0	0	0	0	40*	-
Reading/Washing	0	0	0	0	0	1	0	5300	Forward
New sample	1	0	0	0	0	0	1	4000	Forward
	0	0	1	0	0	0	0	4000	Forward

0/1 = off /on valve state; *elapsed time in seconds.

The flow rate was maintained at 3.0 mL min⁻¹ for each pumping channel, and the assays to determine the optimum operational conditions involved length of reactors, volume of sample zone, time for reaction development (stopped flow), concentration of reagents and acidity of the reacting medium. After settling the appropriate values of the studied variables, and aiming to evaluation the effectiveness of the proposed procedures for tin determination, a set of digested foods samples was processed.

3. Results and discussions

3.1 Sn(IV)-PCV complex

Because the use of a surfactant would improve sensitivity,³² the first assays carried out involved preparation of the pyrocatechol violet solution with and without surfactant addition. The assays were carried out manually, using a 100 mgL⁻¹ Sn(IV) standard solution and two 0.04% PCV (w/v) solutions, one prepared in surfactants medium having the following composition, 0.10 % (v/v) tween-80 and 0.15% (v/v) CTAB solutions and the other without surfactants. After mixing the solutions, the volumes were completed to 25 mL using a 1.0 mol L⁻¹ glycine buffer (pH = 2.0). After development of reaction, the absorption spectra were achieved employing a UV-Vis spectrophotometer (Ocean optics USB 4000). The results are shown in Fig.3.

Figure 3

Analyzing the curve displayed in Fig.3, we observe that the Sn(IV)-PCV complex without surfactants has a maximum absorption at 555 nm, while with surfactants, the maximum absorption shifted to 630 nm. The estimated molar absorptivities are 1.82 x 10³ Lmol⁻¹ cm⁻¹ and 2.81 x 10³ Lmol⁻¹ cm⁻¹ for the first

and second cases, respectively, thereby indicating that the use of surfactant contributed to improve sensitivity.

These results show that the Sn(IV)-PCV complex formed in a medium with a surfactant has a wide absorbing band between the range of 600 to 700 nm, which overlapped the emission band of the LED selected to be the radiation source ($\lambda_{\max} = 630$ nm). Adequate spectra overlapping, is an essential condition to be accomplished, when employing LED as radiation source in photometric measurements.

3.2 Study of the PCV concentration

The effect of the chromogenic reagent solution concentration (PCV) was evaluated between the ranges of 0.01 to 0.08 % (w/v). The assays were carried out using a blank, a 1.0 mg L⁻¹ Sn(IV) standard solution and a surfactants solution consisting of Tween-80 (0.1%) and CTAB (0.15%). The glycine buffer solution was maintained at pH = 2.0. The results are shown in Table 2.

Table 2. Effect of the PCV concentration

PCV concentration (%)	Blank absorbance*	Sn(IV) (1.0 mg L ⁻¹) absorbance*	Δ_{Abs} ** (Net signal)
0.01	0.0010	0.0830	0.0820
0.02	0.0648	0.2060	0.1413
0.04	0.2554	0.4667	0.2113
0.06	0.4449	0.6752	0.2303
0.08	0.5280	0.7845	0.2565

*Average of three replicates; ** Δ_{Abs} = standard solution signal – blank signal

Analyzing the results shown in Table 2, we can deduce that the net signals related to the 1.0 mg L⁻¹ Sn(IV) standard solution, increased three-fold, while measurements made with the blank solution varied from 0.001 to 0.528. As we can see, the 0.08% (w/v) PCV solution generated a blank absorbance that is twofold that achieved using the 0.04 % PCV solution. The net signal for Sn (IV) standard solution was only 18 % lower than that achieved using the higher concentrated PCV solution. Considering that a high blank signal (0.5280)

1
2
3 causes a narrowing of the linear response range, we selected the 0.04 % (w/v)
4 PCV solution for further studies.
5
6

7 8 *3.3. Effect of the pH*

9
10 Because acidity of the reaction medium could affect the Sn(IV)-PCV
11 complex formation, assays were carried out using a blank, and a 1.0 mg L⁻¹
12 Sn(IV) standard solution and a glycine buffer solution prepared at pH ranging
13 from 1.63 to 2.68. The results showed that within the pH range assayed, no
14 significant effect on the signal magnitude was observed. As the literature
15 reports,³⁶ PCV reagent has better selectivity at pH = 2, so this value was
16 selected. The pKa1 of glycine is 2.35, thus it was considered able to afford a
17 good buffering capacity using a 1.0 mol L⁻¹ glycine solution.
18
19
20
21
22
23

24 25 *3.4 Effect of the reaction time*

26 In the flow injection analysis approach, the time interval for reaction
27 development is a function of both flow rate and length of the analytical path. The
28 signal reading step can be performed without the reaction development
29 reaching the equilibrium state. This could become a drawback, when the
30 reaction is slow and high sensitivity must be achieved. Intending to evaluate the
31 reaction time effect on the generated signal, we implemented a stopped flow
32 strategy by interrupting the pumping action for 5.0 s after the sampling step.
33 This time interval was enough to load the flow cell with the sample zone. The
34 experiment was carried out using a 2.0 mg L⁻¹ Sn (IV) standard solution and a
35 0.04% (w/v) PCV solution. The signal reading step was performed for a time
36 interval of 300 s, yielding the results shown in Fig.4.
37
38
39
40
41
42
43
44
45

46
47 Figure 4

48
49 Analyzing this curve, we observe that the signal increased significantly
50 up to the interval of 150 s, showing a tendency towards an equilibrium state at a
51 higher time. This curve allowed us to select the appropriate time interval for
52 reaction development, considering a compromise between sensitivity and
53 sampling rate. Thus, if a higher sensitivity condition was required, a long time
54 interval ($\Delta t = 150$ s) would be selected, whereas the sampling rate would be
55
56
57
58
59
60

1
2
3 reduced. For the subsequent studies, a time interval of 50 s was selected as a
4 compromise to achieve an appropriate sensitivity without lessening the
5 sampling rate.
6
7

8 9 10 *3.5 Effect of the acidity*

11 Since depending on the acidity of the medium, tin underwent
12 hydrolysis,³¹ assays were conducted in order to evaluate the acidity effect. The
13 assays were accomplished by varying from 0.1 to 2.0 mol L⁻¹, the concentration
14 of hydrochloric acid used to prepare the Sn (IV) standard solutions. By taking
15 the slope as the parameter to indicate sensitivity, the results shown that while
16 increasing the acid concentration, an enhancement in sensitivity occurred up to
17 a concentration of 1.00 mol L⁻¹ HCl. Considering that the best linear response (r
18 = 0.999) was achieved with the 0.5 mol L⁻¹ HCl, this solution concentration was
19 selected.
20
21
22
23
24
25
26
27

28 *3.6 Effect of the surfactant concentration*

29 The use of surfactants for the formation of ternary complexes has been
30 reported in the literature,³² as a strategy to increase sensitivity of the analytical
31 methods. This happens due to an increase in molar absorptivity and as well as
32 a wavelength shift towards a higher value.³² Wavelength shift can also help to
33 improve sensitivity, since the signal response of the silicon photodiode
34 increases with wavelength up to 800 nm.
35
36
37
38

39 To evaluate the surfactant effect, the Tween-80 concentration was
40 maintained at 0.10% (v/v), while the CTAB concentration was varied from 0.01
41 to 0.30% (v/v), yielding the curves shown in Fig.5.
42
43
44
45

46
47
48
49
50
51
52
53
54
55
56
57
58
59
60
Figure 5

As we can see, a significant increase in the magnitude of the analytical
signal occurred when the CTAB concentration was increased up to 0.15% (v/v).
The blank measurements decreased throughout, thereby this effect could help
to achieve a wider linear response range, so the 0.15% (v/v) was selected.
Additional assays performed using 0.05, 0.10, 0.20 and 0.40 % (v/v) Tween-80

1
2
3 solutions and results shown that no significant increase in sensitivity occurred,
4 so the 0.10% (v/v) solution was maintained for further assays.
5
6
7

8 9 *3.7 Effect of sample and reagent solution volumes*

10 The syringe pump used to propel solutions in this study, employed a step
11 motor to displace the syringe pistons, which could be programmed to deliver
12 solutions based on the number of rotated steps. This facility was exploited to
13 carry out the sampling step and insertion of reagent solutions into the analytical
14 path. Each syringe has a volume of 10,000 μL . The syringe pump was
15 programed to deliver a volume of 0.25 μL per step corresponding a flow rate of
16 50 $\mu\text{L s}^{-1}$.
17
18
19
20
21

22 When the sampling step was started, the sampling loop (B_1) was filled
23 with the carried solution, thus the standard solution volume pumped through
24 them would be enough to fill it without gradient of concentration. Intending to
25 find the appropriate volume, assays were carried varying the syringe pump
26 rotation steps from 500 up to 2000, thus the volume of solution pumped, varied
27 from 125 up to 500 μL . The results shown an increase around 15 % up to the
28 volume of 375 μL . The volume of sampling loop (Fig.2) was 250 μL , thus this
29 result indicated that te solution volume to assure a complete filling of the
30 sampling loop would be higher than its volume.
31
32
33
34
35
36

37 As depicted in Fig.2, the PCV reagent and surfactants solutions were
38 mixed into the reaction (B_2) prior to add to sample zone. The syringe pump was
39 programmed to deliver volumes of 200, 300 and 400 μL . No significant variation
40 in signal magnitude was observed, so the volume of 300 μL was selected.
41
42
43

44 Carrier fluid was prepared in glycine medium, while sample, PCV reagent
45 and surfactant solutions were prepared water, therefore a poor solutions mixing
46 would case the Schlieren effect,^{33, 34} thus impairing the precision of the
47 measurements. Aiming to evaluate if this effect occurred or not, assays were
48 accomplished using a blank and a 1.0 mgL^{-1} tin solution, yielding the records
49 shown in Fig. 6. The volume of sample zone was 300 μL and the volume of
50 reactor B_3 (Fig. 2) was 250 μL , so that an amount of the solutions mixture
51 attained the flow cell while the sampling step proceeded. Afterwards, syringe
52 pump was halted for 10 s and enabled to run again, in order to displace the
53
54
55
56
57
58
59
60

sample zone through the flow cell. The data acquisition began when sample zone was stopped, thus the first part of both records are practically constant, followed of ascending profiles toward a maximum height. The smoothness of the records profile, and as well as absence of double peaks due to Schlieren effect is an indication that an effective mixing condition was attained.

Figure 6

3.8 Analytical characteristics of the proposed procedure

Once the experimental variables, including volume of sample, reagent solution concentrations, and time interval for reaction had been established, a set of assays was performed in order to evaluate the global performance of the proposed analytical procedure. The results related to figures of merit are summarized in Table 3.

Table 3. Figures of merit

Parameters	
Linear range (mg L ⁻¹ Sn(IV))	0.10 – 1.25
Linear correlation coefficient (r)	0.996
Limit of detection (mg L ⁻¹ Sn(IV))	0.04
Analytical frequency (h ⁻¹)	49
Variation coefficient (%)**	1.30
Consumption of pyrocatechol violet (mg)*	0.058
Sample volume (μL)*	250
Effluent volume (mL)*	2.67
Intra-day RSD (% , n = 4)	1.52
Inter-day RSD (% , n = 4)	3.87

*Value per determination; **Average of 10 consecutive measurements of a 0.35 mgL⁻¹ Sn(IV) standard solution.

The linear response represented by the following equation, absorbance = 0.4211 + 0.3077x was achieved by processing 6 tin standard solutions. The

limit of detection was achieved by applying the 3σ criterion,³⁹ using 10 consecutive measurements of the blank solution.

3.9 Performance Comparison

Intending to evaluate the performance of the propose procedure, we compiled data related to tin determination from some existing procedures that are shown in Table 4.

Among the parameters displayed in this table, we observe that limit of detection of the proposed procedure is not so low as those of the references 6, 36 and 39. Nevertheless, the current procedure offers other appreciable advantages, including high throughput, low consumption of reagent, and low volume of waste generation. Furthermore, the limit of detection is twenty times lower than the value established by the regulatory agency,¹⁵ which was achieved without any pre-concentration step.

Table 4. Performance comparison

Proce dure	Strategy for increased sensitivity	Linear range	Limit of detection ($\mu\text{g L}^{-1}$)	Sampling Rate (Det h ⁻¹)*	Effluent (mL)**	Ref.
MSFIA	Long pathlength flow cell	0.10 - 1.25 (mg L ⁻¹)	40	49	2.0	Proposed procedure
FIA	Solid phase	2 - 40 ($\mu\text{g L}^{-1}$)	0.3	7.2	10	41
FIA	Surfactant	0.04 - 5.00 (mg L ⁻¹)	40	30	8.4	40
Batch wise	Surfactants	0 - 1.20 (mg L ⁻¹)	7	-	50***	38
Batch wise	Surfactants	0.1 – 2.5 (mg L ⁻¹)	18	-	10***	20
Batch wise	Kinetic	0.1–1.80 (mg L ⁻¹)	30	-	5***	21
Batch wise	Cloud point extraction	0.30 – 175.00 ($\mu\text{g L}^{-1}$)	0.16	-	10***	6

*Determination per hour; **Value per determination; ***Calculated using data taken from references.

3.10 Study of potential interferences

Evaluation of the potential interferences on the proposed procedure was performed, using a 0.5 mg L⁻¹ Sn(IV) standard solution with and without the potential interfering. The results are shown in Table 5. A variation of $\pm 5.0\%$ in the analytical signal was taken as the criterion to define if interference had occurred or not. Analyzing these results, we observe that only Fe³⁺ presented significant interference at a concentration 10 times higher than the reference concentration. This occurred because Fe³⁺ cation also reacts with PCV and forms a stable complex.³⁸ This reagent does not react with Fe²⁺, thus offering a way to overcome the interference effect exploiting this feature. Using this information, further assays were performed using a 0.2 mol L⁻¹ ascorbic acid solution. An aliquot of this solution (200 μ L) was added to 10 mL of a 0.5 mg L⁻¹ Sn(IV) standard solution containing Fe³⁺. The results show that the iron interference effect was overcome, so that a Fe³⁺ concentration, 600 times greater than the Sn⁴⁺ did not cause any significant effect.

Table 5. Results concerning to potential interfering species

Evaluated Species	Concentration/ratio [X]*/[Sn (IV)]	Interference (%)
Co ²⁺	2000	<5
Na ²⁺	2000	<5
Ni ²⁺	400	<5
Mg ²⁺	2000	<5
K ⁺	400	<5
Cd ²⁺	100	<5
Mg ²⁺	2000	<5
Zn ²⁺	2000	<5
Cu ²⁺	20	<5
Al ³⁺	100	<5
V ⁵⁺	100	<5
Fe ³⁺	20	9.45

*[X] = concentration of the assayed chemical specie.

3.11 Tin determination in food samples

Aiming to verify if the cans used for food storage did or did not have a tin coating, a set of assays was performed using the Laser Induced Breakdown Spectroscopy (LIBS) methodology.^{42,43} The assays were carried out by applying several shots at different points on a fragment of a can as depicted in Fig.7. The spectra records show that the cans have a tin coat. Each can was divided in three parts: top, middle and bottom. The results show that there was not a homogenous tin distribution. This feature was observed for all cans used in this work.

Figure 7

The tin found in the cans could have leached to the foods. To determine the presence of tin in the food, samples were digested using microwave-assisted methodology as described in the experimental section. To test accuracy, they were also analyzed employing Inductively Coupled Plasma Optical Emission Spectrometry (ICP OES). The results are shown in Table 6. The limit of detection the reference method was 0.14 mg L⁻¹ Sn. Only one sample had a concentration higher than this value, thus the standard addition methodology was applied in order to evaluate the accuracy of the proposed procedure. Analyzing the results shown in Table 6, we observed that a recovery between the range of 95 to 110 % was achieved, which would be considered satisfactory.

Table 6. Results comparison.

Sample	Reference method (mg L ⁻¹)	Proposed method (mg L ⁻¹)	Added (mg L ⁻¹)	Found (mg L ⁻¹)	Recovery (%)
Grated tuna	<LOD	0.14 ± 0.09	0.2	0.33 ± 0.06	95
Vegetable corn	<LOD	0.11 ± 0.07	0.2	0.30 ± 0.08	95
Tomato extract	<LOD	0.16 ± 0.07	0.2	0.38 ± 0.06	110
Tomato without skin	0.42 ± 0.07	0.44 ± 0.04	0.2	0.63 ± 0.01	95

Tomato extract	<LOD	0.20 ± 0.02	0.2	0.40 ± 0.05	99
----------------	------	-------------	-----	-------------	----

Each result is the average of measurements performed using three replicates of each sample.

4. Conclusions

The proposed procedure afforded a limit of detection 0.04 mg L⁻¹ Sn(IV), which is twenty times lower than the reference value established by the European Community Regulatory Commission.¹⁴ This result indicates that the LED based photometer furnished with flow cell with a long optical path length, constitutes a useful and cost effective alternative for Sn determination in canned food.

The use of a multi-syringe module for fluid propelling, combined with a flow manifold designed based on the multicommutation approach, afforded facilities to develop this analytical procedure with positive features such as high sampling throughput, low reagent consumption and low volume of waste generation, making the procedure environmental friendly as requested by the green chemistry guidelines.^{29,30}

Acknowledgements

The authors acknowledge financial support from CNPq, INCTAA, FAPESP and CAPES.

References

- 1 B. M. Mahan, R. J. Myers, *Química: um curso universitário*. São Paulo: Edgard Blucher, **2003**.
- 2 C. A. L. Filgueiras, *Química nova*, **1998**, 21, 176.
- 3 N. N. Greenwood, A. Earnshaw, *Chemistry of the elements*. Oxford: Pergamon Press, **1984**.
- 4 P. Quevauviller, R. Lavigne, R. Pinel, M. Astruc, *Environmental Pollution*, **1989**, 57, 149.

- 1
2
3 5 E. A. Ostrakhovitch, M. G. Cherian, *Handbook on the toxicological of metals:*
4 *tin*. (3th ed.). Amsterdam: Academic Press, (Chapter 42), **2007**.
5
6
7 6 T. Madrakian, F. Ghazizadeh, *Journal of the Brazilian Chemical Society*,
8 **2009**, 20, 1535.
9
10
11 7 S. Blunden, T. Wallace, *Food and cosmetics toxicology*, **2003**, 41, 1651.
12
13 8 U.S. Department of health and human services. Public Health Service Agency
14 for Toxic Substances and Disease Registry. [http://www.atsdr.cdc.gov/tfacts55.p](http://www.atsdr.cdc.gov/tfacts55.pdf)
15 [df](http://www.atsdr.cdc.gov/tfacts55.pdf). Accessed in: April, 23th 2014.
16
17 9 L. Perring, M. Basic-Dvorzak, *Analytical and Bioanalytical Chemistry*, **2002**,
18 374, 235.
19
20 10 S. Shimbo, T. Watanabe, H. Nakatsuka, K. Yaginuma-Sakurai, M. Ikeda,
21 *Environmental Health and Preventive Medicine*, **2013**, 18, 230.
22
23 11 R. A. Brown, C. M. Nazario, R. S. Tirado, J. Castrillon, E. T. Agard,
24 *Environmental Research*, **1977**, 13, 56.
25
26
27 12 M. Amjadi, J. L. Manzoori, V. Hamedpour, *Food Analytical Methods*, **2013**, 6,
28 1657.
29
30
31 13 Brazillian Health Surveillance Agency – ANVISA, *Lei nº 9.832, 14 de*
32 *setembro de 1999*, Brasil: Brasília.
33
34
35 14 European Commission, *Setting maximum levels for certain contaminants in*
36 *foodstuffs nº 1881/2006*. Paris: European Commission.
37
38
39 15 World Health Organization, Evaluation of certain food additives and
40 contaminants, 2001 (WHO technical report series, 901).
41
42
43 16 M. Welna, A. Szymczycha-Madeja, *Food Analytical Methods*, **2014**, 7, 127.
44
45
46 17 C. G. Yuan, G. B. Jiang, B. He, J. F. Liu, *Microchimica Acta*, **2005**, 150, 329.
47
48
49 18 J. H. Mendez, B. M. Cordero, R. C. Martinez, L. G. Davila, *Microchemical*
50 *Journal*, **1987**, 35, 288.
51
52
53 19 Z. H. Yu, J. Sun, M. Jing, X. Cao, F. Lee, X. R. Wang, *Food chemistry*, **2010**,
54 119, 364.
55
56
57 20 X. R. Huang, W. J. Zhang, S. H. Han, X. Q. Wang, *Talanta*, **1997**, 44, 817.
58
59
60 21 T. Madrakian, A. Afkhami, R. Moein, M. Bahram, *Talanta*, **2007**, 72, 1847.

- 1
2
3 22 J. Ruzicka, E. H. Hansen, *Analytica Chimica Acta*, **1975**, 78, 145.
4
5 23 J. Ruzicka, G. D. Marshall, *Analytica Chimica Acta*, **1990**, 237, 329.
6
7 24 B. F. Reis, M. F. Giné, E. A. G. Zagatto, J. L. F. C. Lima, R. A. Lapa,
8
9 *Analytica Chimica Acta*, **1994**, 293, 129.
10
11 25 L. Chaparro, L. Ferrer, L. Leal, V. Cerdà, *Talanta*, **2015**, 133, 94.
12
13 26 C. Henríquez, H. Horstkotte, V. Cerdà, *International Journal of*
14
15 *Environmental Analytical Chemistry*, **2013**, 93, 1236.
16
17 27 F. R. P. Rocha, B. F. Reis, E. A. G. Zagatto, J. L. F. C. Lima, R. A. S. Lapa,
18
19 J. L. M. Santos, *Analytica Chimica Acta*, **2002**, 468, 119.
20
21 28 S. S. M. Rodrigues, J. L. M. Santos, *Talanta*, **2012**, 96, 210.
22
23 29 S. Garrigues, S. Armenta, M. de la Guardia, *Trends in Analytical Chemistry*,
24
25 **2010**, 29, 592.
26
27 30 W. R. Melchert, B. F. Reis, F. R. P. Rocha, *Analytica Chimica Acta*, **2012**,
28
29 714, 8.
30
31 31 W. J. Ross, J. C. White, *Analytical Chemistry*, **1961**, 33, 421.
32
33 32 H. B. Corbin, *Analytical Chemistry*, **1973**, 45, 534.
34
35 33 E. A. G. Zagatto, M. A. Z. Arruda, A. O. Jacintho, I. L. Mattos, *Analytica*
36
37 *Chimica Acta*, **1990**, 234, 153.
38
39 34 S. R. B. Santos, M. C. U. Araújo, R. A. Barbosa, *Analyst*, **2002**, 127, 324.
40
41 35 F. G. Santos, A. C. Pereira, S. M. Cruz, C. A. Bizzi, E. M. M. Flores, B. F.
42
43 Reis, *Analytical Methods*, **2015**, 7, 4769.
44
45 36 T. R. Dias, M. A. S. Brasil, M. A. Feres, B. F. Reis, *Sensors and Actuators B*,
46
47 **2014**, 198, 448.
48
49 37 A. Fonseca, I. M. Raimundo, *Analytica Chimica Acta*, **2004**, 522, 223.
50
51 38 A. C. S. Costa, L. S. G. Teixeira, S. L. C. Ferreira, *Talanta*, **1995**, 42, 1973.
52
53 39 L. A. Currie, *Analytical Chemistry*, **1968**, 40, 586.
54
55 40 X. Zou, Y. Li, M. Li, B. Zheng, J. Yang, *Talanta*, **2004**, 62, 719.
56
57
58
59
60

1
2
3 41 L. F. Capitain-Vallvey, M. C. Valencia, G. Mirón, *Analytica Chimica Acta*,
4 **1994**, 289, 365.

5
6
7 42 L. C. Nunes, J. W. B. Braga, L. C. Trevizan, P. F. Souza, G. G. A. Carvalho,
8 D. Santos, R. J. Poppi, F. J. Krug, *Journal of Analytical Atomic Spectrometry*,
9 **2010**, 25, 1453.

10
11
12 43 D. Santos Junior, L. V. G. Tarelho, F. J. Krug, D. M. B. P. Milor, L. Martin
13 Neto, N. D. Vieira Junior, *Revista Analytica*, **2006**, 24, 72.
14
15
16
17
18
19
20
21
22
23
24
25
26
27
28
29
30
31
32
33
34
35
36
37
38
39
40
41
42
43
44
45
46
47
48
49
50
51
52
53
54
55
56
57
58
59
60

Caption of figures

Figure 1. Diagram of the LED based photometer. Tr = BC547; LED = light emitting diode, $\lambda = 630$ nm; I_1 and I_2 = radiation beams coming from the LED at flow cell and leaving the flow cell towards the photodetector, respectively; gc = glass cylinders, 20 mm long and 1,2 mm diameter; fe = flow cell body, glass tube 1.2 mm inner diameter; x = flow cell length, 200 mm; f = fused surfaces; Det = photodetector, OPT301; S_0 = generated signal (mV); in and out = solution input and output, respectively.

Figure 2. Diagram of the flow system module. M = syringe pump module; $S_1 - S_4$ = syringes; $V_{B1} - V_{B4}$ = three-way solenoid valves of the syringe pump; $V_1 - V_3$ = three-way solenoid valves; B_1, B_2 and B_3 = sampling loop and reactor coils of polyethylene tube, 0.8 mm inner diameter and 50, 25 and 50 cm long, respectively; $C_1 - C_3$ = confluences; Det = photometry unit detection.

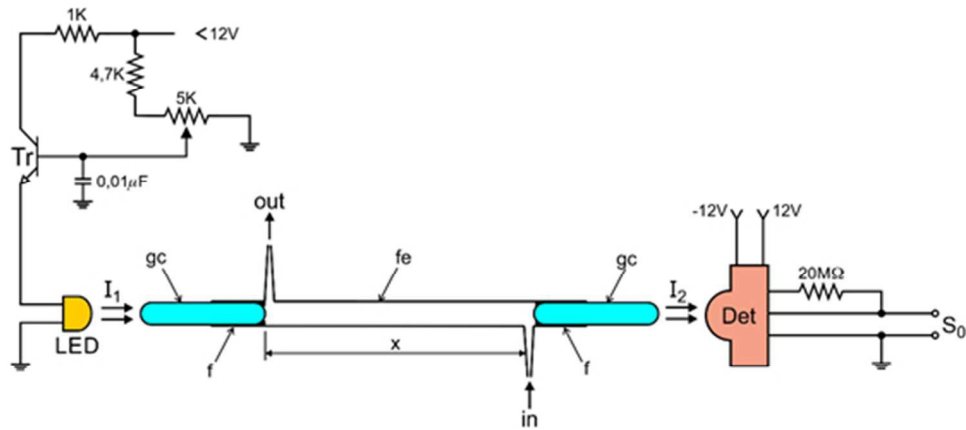
Figure 3. Absorption spectra of the Sn(IV)-PCV complexes.

Figure 4. Effect of the stopped flow delay time.

Figure 5. Effect of the surfactant concentration. Curves *a* and *b* correspond to the blank and a 1.0 mg L^{-1} Sn (IV) standard solution, respectively.

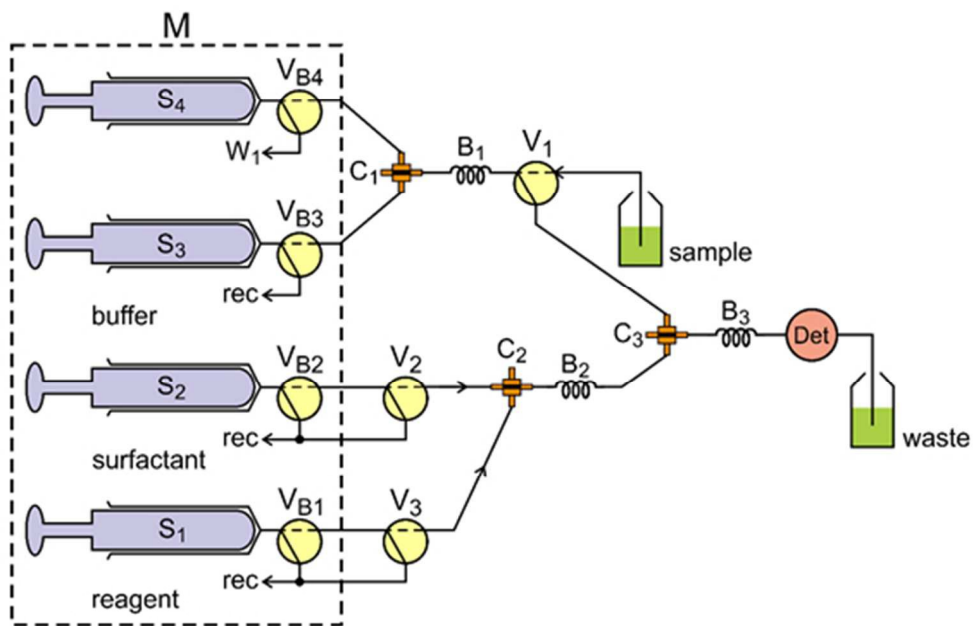
Figure 6. Records of the measurements. From right records of blank and a 1.0 mgL^{-1} tin solution.

Figure 7. Searching for tin in a can fragment. From the left, view of the can fragment after laser ablation and tin emission spectra. Records labeled as *a*, *b* and *c* correspond to laser ablation performed on the top, middle and bottom of the can.



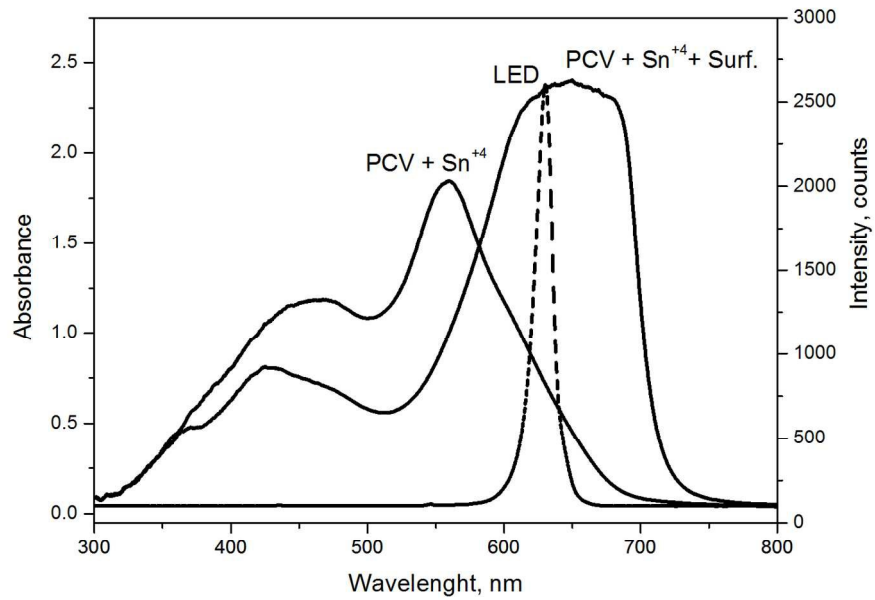
154x71mm (96 x 96 DPI)

1
2
3
4
5
6
7
8
9
10
11
12
13
14
15
16
17
18
19
20
21
22
23
24
25
26
27
28
29
30
31
32
33
34
35
36
37
38
39
40
41
42
43
44
45
46
47
48
49
50
51
52
53
54
55
56
57
58
59
60

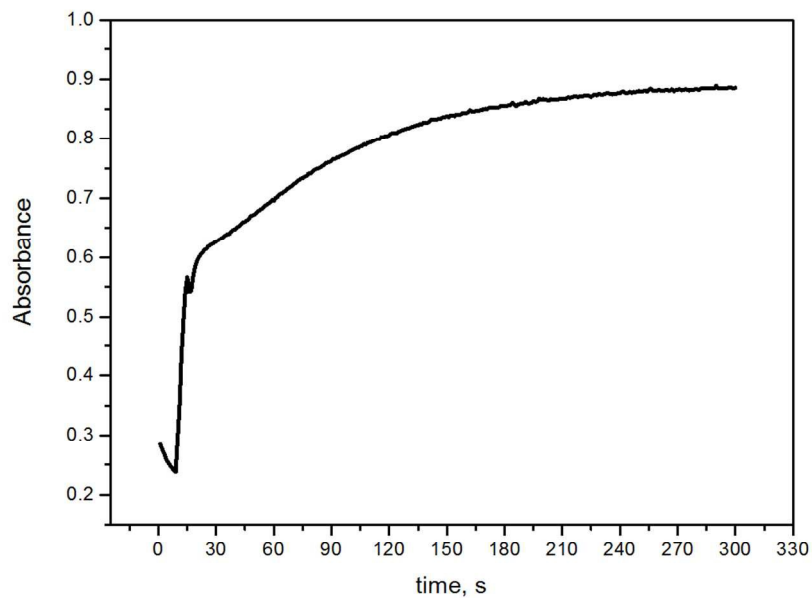


153x101mm (96 x 96 DPI)

1
2
3
4
5
6
7
8
9
10
11
12
13
14
15
16
17
18
19
20
21
22
23
24
25
26
27
28
29
30
31
32
33
34
35
36
37
38
39
40
41
42
43
44
45
46
47
48
49
50
51
52
53
54
55
56
57
58
59
60

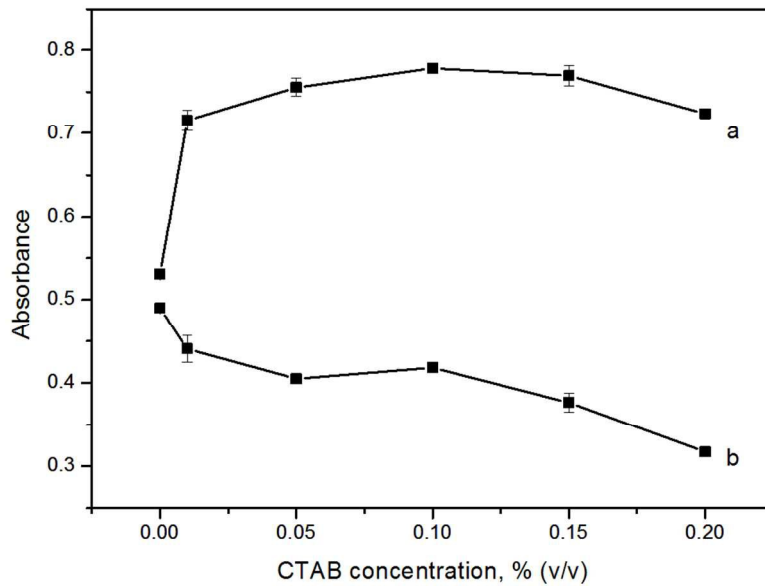


283x199mm (150 x 150 DPI)



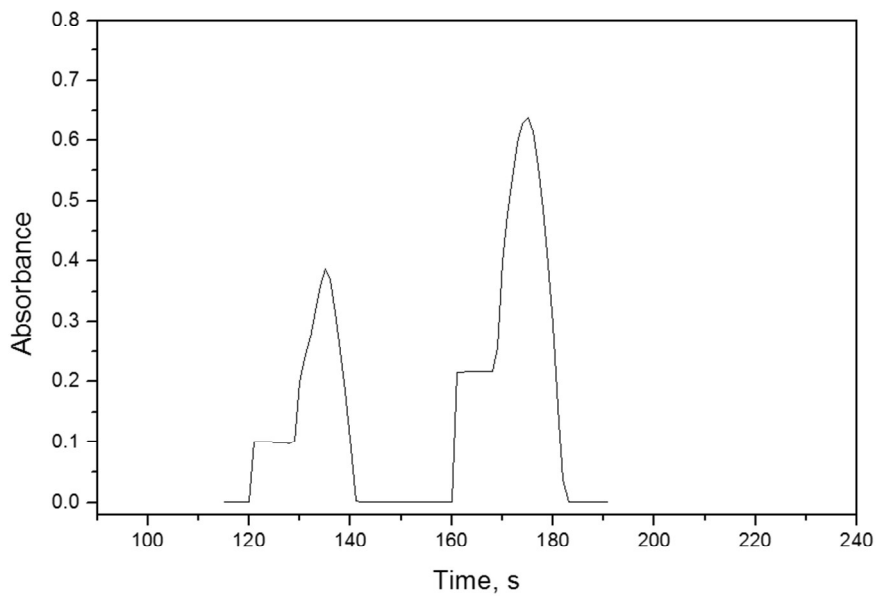
212x150mm (150 x 150 DPI)

1
2
3
4
5
6
7
8
9
10
11
12
13
14
15
16
17
18
19
20
21
22
23
24
25
26
27
28
29
30
31
32
33
34
35
36
37
38
39
40
41
42
43
44
45
46
47
48
49
50
51
52
53
54
55
56
57
58
59
60



215x150mm (150 x 150 DPI)

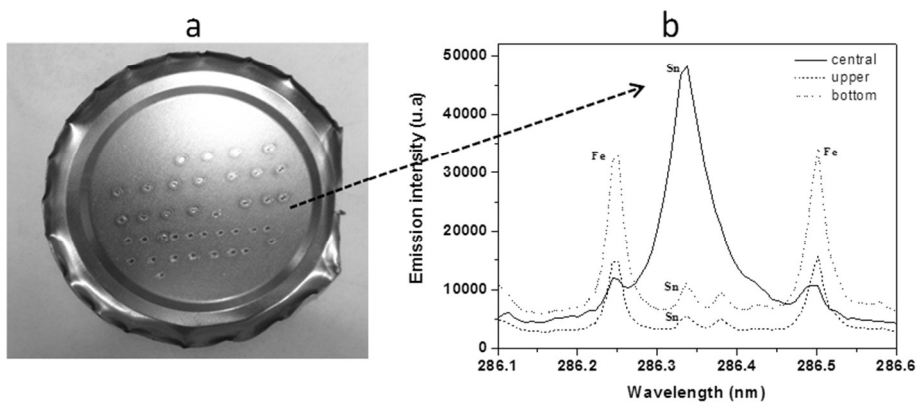
1
2
3
4
5
6
7
8
9
10
11
12
13
14
15
16
17
18
19
20
21
22
23
24
25
26
27
28
29
30
31
32
33
34
35
36
37
38
39
40
41
42
43
44
45
46
47
48
49
50
51
52
53
54
55
56
57
58
59
60



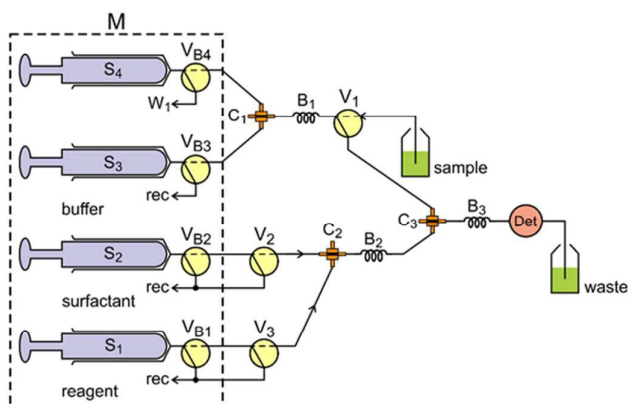
171x124mm (150 x 150 DPI)

1
2
3
4
5
6
7
8
9
10
11
12
13
14
15
16
17
18
19
20
21
22
23
24
25
26
27
28
29
30
31
32
33
34
35
36
37
38
39
40
41
42
43
44
45
46
47
48
49
50
51
52
53
54
55
56
57
58
59
60

1
2
3
4
5
6
7
8
9
10
11
12
13
14
15
16
17
18
19
20
21
22
23
24
25
26
27
28
29
30
31
32
33
34
35
36
37
38
39
40
41
42
43
44
45
46
47
48
49
50
51
52
53
54
55
56
57
58
59
60



245x108mm (96 x 96 DPI)



Graphical abstract. Diagram of the flow system module at the stand by condition.